Plant Cell Tiss Organ Cult (2016) 125:353–374
DOI 10.1007/s11240-016-0956-y

ORIGINAL ARTICLE

DNA methylation and proteome profiles of *Araucaria angustifolia* (Bertol.) Kuntze embryogenic cultures as affected by plant growth regulators supplementation

Hugo P. F. Fraga[1] · Leila N. Vieira[1] · Angelo S. Heringer[2] · Catarina C. Puttkammer[1] · Vanildo Silveira[2] · Miguel P. Guerra[1]

Received: 12 September 2015 / Accepted: 5 February 2016 / Published online: 11 February 2016

Abstract *Araucaria angustifolia* is a critically endangered conifer native to South America, and somatic embryogenesis (SE) is one of the most promising biotechnological tools for its conservation and mass propagation. In vitro tissue culture and chemical compounds supplemented to culture medium, especially plant growth regulators (PGRs), are known to affect DNA methylation and protein expression profiles, modulating the phenotype and/or the embryogenic potential. Here, we evaluated the global DNA methylation (GDM) levels of *A. angustifolia* embryogenic cultures (EC) during SE induction and multiplication steps for 1 year subcultures, and identified a wide range of differentially expressed proteins in PGR-free or -supplemented treatments. During long-term subcultures, PGR-supplementation proved to gradually increase the GDM, which may compromise genomic stability and evoke gene expression modifications. Label-free proteomics enabled a robust protein identification and quantification in *A. angustifolia* EC. Exclusively expression of PIN-like protein in PGR-supplemented treatment indicated a possible differential response of the EC to polar auxin transport, which can generate implications in its morphogenetic response to maturation step. Up-regulation of stress-related proteins in EC from PGR-supplemented treatment suggests its more stressful environment, triggering notable responses to hormonal, osmotic and oxidative stresses. Improved expression of proteins involved with protein folding and stabilization processes in PGR-free treatment could play a protective function in response to stress conditions caused by in vitro culture, and may provide an adaptive advantage to these EC. The expression of several proteins associated to terpenoid biosynthesis suggests that EC from both treatments and cell lines are possibly producing these compounds.

Keywords Label-free proteomics · Somatic embryogenesis · Epigenetics · Stress-related proteins · Terpenoid biosynthesis

Introduction

Araucaria angustifolia is a dioecious perennial conifer native to South America, occurring in South and Southeastern Brazil, and restricted areas of Northwestern Argentina and Paraguay (Guerra et al. 2008). Drastic population decline and habitat reduction culminated in the inclusion of *A. angustifolia* on the IUCN international list as "critically endangered" (www.iucnredlist.org). Many efforts have been carried out in order to propagate and conserve this species; however, conventional strategies are hampered mostly due to the recalcitrant nature of the seeds (Salmen-Espindola et al. 1994; Panza et al. 2002). Micropropagation techniques, such as somatic embryogenesis (SE), have potential for clonal propagation and ex situ conservation of commercial and endangered plant species,

Electronic supplementary material The online version of this article (doi:10.1007/s11240-016-0956-y) contains supplementary material, which is available to authorized users.

✉ Miguel P. Guerra
miguel.guerra@ufsc.br

[1] Laboratório de Fisiologia do Desenvolvimento e Genética Vegetal, Centro de Ciências Agrárias, Universidade Federal de Santa Catarina, Florianópolis, SC 88034-001, Brazil

[2] Laboratório de Biotecnologia, Centro de Biociências e Biotecnologia, Universidade Estadual do Norte Fluminense Darcy Ribeiro, Campos dos Goytacazes, RJ 28013-602, Brazil

especially conifers (Guerra et al. 2000; Klimaszewska et al. 2011; Jo et al. 2013).

Somatic embryogenesis is the developmental restructuring of somatic cells toward the embryogenic pathway, and forms the basis of cellular totipotency in higher plants (Karami and Saidi 2010). Unlike zygotic embryos, somatic embryos can be easily manipulated and growing conditions can be controlled. These features make the SE an efficient model system for the study of morphological, physiological, molecular and biochemical aspects that occur during the initiation and development in higher plants (Zhang et al. 2007; Karami and Saidi 2010).

The early SE process in *A. angustifolia* is well characterized by the development of embryogenic cultures (EC), which, in turn, are multiplied as pro-embryogenic masses (PEM) during the early stages of SE. This step is successfully achieved; however, unknown factors hamper further somatic embryos maturation from PEM (Santos et al. 2008, 2010; Vieira et al. 2012). Recently, promising results were achieved with EC induced and proliferated in plant growth regulators-free (PGR-free) culture medium, generating somatic embryos in advanced maturation stages with reproducibility (Fraga et al. 2015). Although these recent advances, there are still several bottlenecks that require a better understanding of the underlying causes.

Ontogenetic development in trees is characterized by successive phase changes which are accompanied by drastic morphological, biochemical and physiological modifications (Poethig 1990; Teyssier et al. 2014). Cell differentiation and development are controlled by means of temporal and spatial activation and silencing of specific genes (Noceda et al. 2009). Among the mechanisms involved in the regulation of plant development, DNA methylation, a pivotal epigenetic mechanism, is one of the key factors controlling gene/protein expression (Feng et al. 2010; Miguel and Marum 2011). In cell and tissue culture systems, differentiation and dedifferentiation processes, as well as cell division, are followed by methylation and demethylation events in genomic DNA tissue-specific (Msogoya et al. 2011).

In vitro tissue culture techniques and chemical compounds supplemented to culture medium, especially PGRs, are known to induce modifications in global DNA methylation (GDM) levels, which may ultimately affect the phenotype and/or the embryogenic potential (LoSchiavo et al. 1989; Valledor et al. 2007; Rodríguez-López et al. 2010). Specific changes in GDM in plants were proved to be related to the developmental phase (Fraga et al. 2002), being also possible to relate the specific methylation status to the further in vitro morphogenic ability of EC (Valledor et al. 2007). Several recent reports on SE of different conifer species have suggested causal relationships between GDM levels and in vitro morphogenetic competence (Klimaszewska et al. 2009; Noceda et al. 2009; Leljak-Levanic et al. 2009; Teyssier et al. 2014).

Proteomic studies have been shown to be powerful tools for monitoring the physiological status of plant organs under specific developmental conditions (Rose et al. 2004). Proteins directly influence cellular biochemistry, providing more accurate analysis of cellular changes during growth and development (Chen and Harmon 2006). Unlike model biological systems, the full potential of proteomics is far from being fully exploited in plant biology research (Abril et al. 2011). Thus, only a low number of plant species have been investigated at the proteomics level and, mainly, by using strategies based on 2-DE coupled to MS, resulting in low proteome coverage (Carpentier et al. 2008).

Proteomic analysis during SE of woody species have been reported (Marsoni et al. 2008; Cangahuala-Inocente et al. 2009; Pan et al. 2009, 2010; Sghaier-Hammami et al. 2010). Recently, efforts have been made to describe *A. angustifolia* somatic and zygotic embryogenesis at the molecular level, using proteomic and transcriptomic approaches (Balbuena et al. 2009, 2011; Jo et al. 2013; Elbl et al. 2015). *A. angustifolia* is a non-model conifer, for which bioinformatic resources are scarce or even absent; consequently, protein identification mostly relies on limited sequence coverage. In addition, little information about non-Pinaceae conifer species is available in the database.

The multidimensional protein identification technology "MudPIT" has become a popular approach for performing shotgun proteomics, with high resolution orthogonal separation coupled to tandem mass spectrometry (2D-nanoLC-MS/MS) (Chen et al. 2006; Heringer et al. 2015). High-definition HDMS^E (data independent acquisition with ion mobility) (Lalli et al. 2013), with increased selectivity and specificity, are required for shotgun proteomics and complex samples due to their resolving power for overlapping chimeric peptides (Geromanos et al. 2009). This technology has enabled the identification of low-abundant proteins, which are often missed when using two-dimensional electrophoresis (Washburn et al. 2001). Here, we describe for the first time for *A. angustifolia* a 2D-nanoLC-MS/MS strategy for proteome investigation.

A remarkable aspect in the induction and maintenance process of *A. angustifolia* EC is the possibility of establishing cell lines both in the presence or absence of PGR supplementation to culture medium. This striking ability allows the establishment of a reliable model system to investigate the possible effects of these PGRs in both GDM levels and proteome profile of EC, with minimal biological variation. In this sense, the aim of the present work was to investigate the involvement of individual proteins in response to PGR supplementation during EC proliferation and to identify the wide range of proteins that are differentially regulated in these different treatments (PGR-free

or –supplemented). We used the HDMS^E technique, a gel- and label-free approach which allows the qualitative and quantitative analysis of large number of protein in complex samples. In addition, we quantified the GDM levels of EC induced and maintained in PGR-free or -supplemented treatments for 1 year subculture.

Materials and methods

Plant material

Immature female cones bearing early globular-staged zygotic embryos were collected in December 2012, from an *A. angustifolia* open-pollinated natural population in Lages, Santa Catarina–Brazil (latitude 28°02′S, longitude 50°17′W, altitude 1030 m). Three different female individuals were chosen as donor plants (Cr01, Cr02, and Cr03). Two independent cones were collected from each donor plant, wherein one cone was used to establish an individual cell line (named Cr01, Cr02, and Cr03 according to the respective donor plant), and the other one for GDM analysis.

Somatic embryogenesis induction and EC proliferation

Embryogenic cultures were induced according to Santos et al. (2002). The seeds were submitted to disinfestation procedures with 70 % ethanol for 5 min and 1.5 % sodium hypochlorite for 15 min, followed by a triple-washed with autoclaved distilled water. Zygotic embryos were excised and inoculated in Petri dishes containing 25 mL of induction culture medium. The basic induction culture medium consisted of BM macro-, micro-salts and vitamins (Gupta and Pullman 1991) containing L-glutamine (1.0 g L^{-1}), myo-inositol (1.0 g L^{-1}), casein hydrolysate (0.5 g L^{-1}), and sucrose (30 g L^{-1}). Two different induction treatments were established: PGR-free induction culture medium (BM_0), and PGR-supplemented induction culture medium (4 µM 2,4-D, 2 µM BAP, 2 µM KIN—BM_4). All culture media were gelled with Phytagel® (2 g L^{-1}), the pH adjusted to 5.8 and autoclaved at 121 °C, 1.5 atm for 15 min. All the cultures were maintained in a growth room in the absence of light at temperature of 22 ± 2 °C.

After 30 days induction, the EC obtained were subcultured in Petri dishes containing 25 mL of BM_0 or BM_2 (2 µM 2,4-D, 0.5 µM BAP, 0.5 µM KIN), according to the respective induction culture media composition (with or without PGR supplementation). Subcultures were made every 21 days in gelled BM_0 or BM_2 culture medium. All the cultures were maintained in a growth room in the absence of light at temperature of 22 ± 2 °C.

Global DNA methylation analysis

Samples for GDM analysis were collected from the three different *A. angustifolia* lines (Cr01, Cr02, and Cr03), wherein each line were considered as a biological replicate. These samples consisted of: (a) early globular-staged zygotic embryos (explant used for SE induction); (b) EC after 30 days induction in culture media BM_0 or BM_4; (c) EC derived from multiplication in BM_0 or BM_2 culture media, every two multiplication cycles, from cycle 3 to cycle 17, totaling a period of 1 year collections (Fig. 1). The aim of such sampling was to follow up the dynamics of global DNA methylation in EC induced and long-term maintained in PGR presence or absence.

DNA extraction was performed in samples consisting of three different biological replicates (Cr01, Cr02 and Cr03 cell lines), for each collection time, according to Doyle (1987). Nucleic acids digestion procedures were based on the method described by Johnston et al. (2005) and Fraga et al. (2012). HPLC analysis was performed according to Johnston et al. (2005). A HyperClone™ 5 µm ODS (C18) 120 Å, LC Column 250 × 4.6 mm (Phenomenex®, Torrance, USA), guard column (4.0 × 3.0 mm) (Phenomenex®), and UV detector (280 nm) were used. The gradient program consisted of 3 min with 100 % buffer A (0.5 % v/v methanol in 10 mM KH_2PO_4 adjusted to pH 3.7 with phosphoric acid, 0.22 µm filtered), followed by a linear gradient from 3 to 20 min to 100 % of buffer B (10 % v/v methanol in 10 mM KH_2PO_4 adjusted to pH 3.7 with phosphoric acid, 0.22 µm filtered), followed by 20–25 min with 100 % of buffer B. A flow rate of 1 mL min^{-1} and 20 µL of sample injection volume were applied.

The dNTPs (Fermentas®, Hanover, MD, USA) used as standards (dA, dT, dC and dG) and 5mdC were digested for 2 h with alkaline phosphatase (10 U mL^{-1}) and Tris-HCl (0.5 M, pH 8.3) at 37 °C to obtain the nucleosides. The standard nucleosides (5–50 mM) were prepared in deionized H_2O and stored at −20 °C. 5mdC quantification (%) was performed according to 5mdC concentration divided by 5mdC concentration plus dC concentration multiplied by 100. The obtained peak area was analyzed by LC Solution software (Shimadzu®, Kyoto, Japan). Data were analyzed by Statistica® (Statsoft Inc., Tulsa, USA) for Windows® version 7.0 and submitted to ANOVA. Treatments were compared by Student–Newman–Keuls (SNK) post hoc test ($p < 0.05$).

Proteomic analyses

Total protein extraction

Embryogenic cultures from Cr01 and Cr02 cell lines established in PGR-free and –supplemented culture media

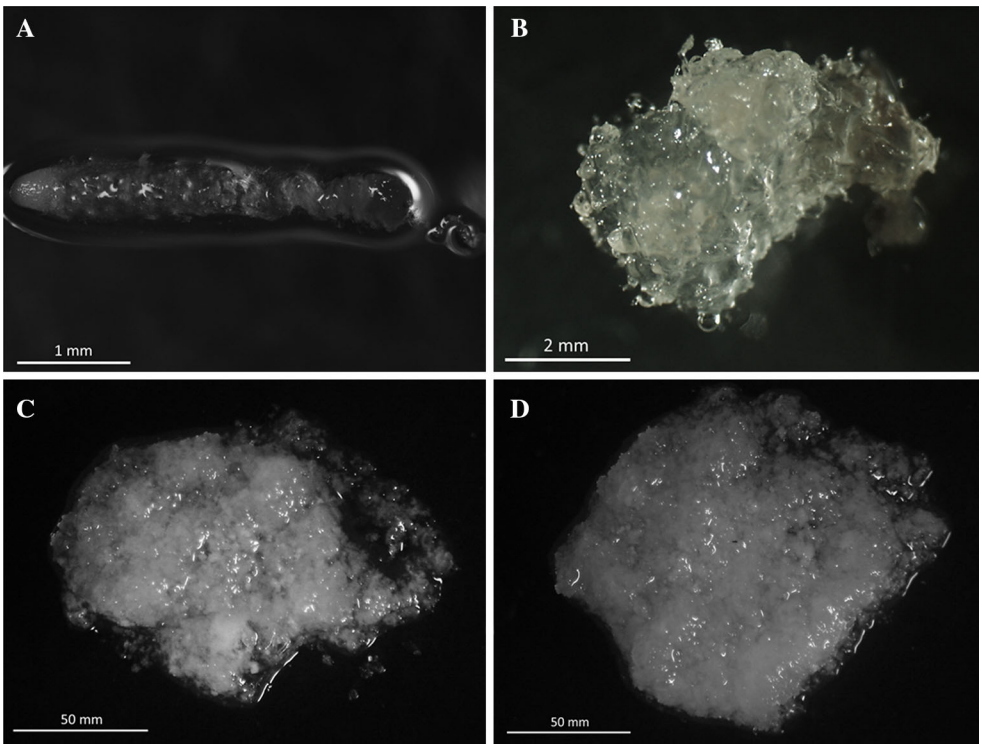

Fig. 1 Morphological features of plant material used for DNA methylation and proteomic analyses. **a** Early globular-staged *A. angustifolia* zygotic embryos (explant used for somatic embryogenesis induction); **b** representative embryogenic culture (EC) obtained after 30 days culture in induction culture media; **c** representative EC derived from plant growth regulators-free treatment during multiplication step; **d** representative EC derived from plant growth regulators-supplemented treatment during multiplication step

were collected after seven cycles in multiplication step and subjected to total protein extraction (Fig. 1c, d). Protein extracts were prepared in biological triplicate (500 mg FM) for each treatment (PGR-free or –supplemented) in each cell line evaluated. Protein extraction protocol used was based on that described by Balbuena et al. (2009). Briefly, the samples were ground and transferred to clear 2-mL microtubes containing 1.5 mL of extraction buffer (7 M urea, 2 M thiourea, 1 % DTT, 2 % Triton X-100, 0.5 % Pharmalyte, 1 mM PMSF, all reagents purchased from Sigma-Aldrich). The extracts were briefly vortexed and kept in extraction buffer on ice for 30 min followed by centrifugation at 12,000*g* for 5 min at 4 °C. The supernatants were collected, and protein concentration was measured using a 2-D Quant Kit (GE Healthcare, Piscataway, NJ, USA). The five protein extracts resulting from each treatment were pooled, totaling 100 µg of protein (Luge et al. 2014). The samples were stored at −20 °C until proteomic analysis.

Protein digestion

The protein samples (100 µg) were purified using a methanol–chloroform method according to Komatsu et al. (2013). Briefly, 600 µL methanol and 150 µL chloroform was added and the sample was mixed by vortexing. Then, 450 µL water was added to the sample to induce phase separation, mixed by vortexing, and centrifuged at 20,000×*g* for 10 min at room temperature. The upper phase was carefully discarded, and 450 µL methanol was then added slowly to the remaining organic phase. The samples were centrifuged again with the same conditions, the supernatant was removed, and the pellet was dried in air for 10 min. The dried pellet was resuspended in 50 µL 50 mM NH_4CO_3.

For trypsin digestion, a 2 µg μL^{-1} solution of 50 µL of the previous sample plus 25 µL of 0.2 % v/v *Rapi*GEST (Waters, USA) (Yu et al. 2003) was added to a 1.5-mL microfuge tube, vortexed and heated in an Eppendorf Thermomixer Comfort device at 80 °C for 15 min. Then, 2.5 µL of 100 mM DTT was added and placed in the thermomixer at 60 °C for 30 min. The tubes were placed on ice (30 s), and 2.5 µL of 300 mM iodoacetamide (IAA) was added, followed by vortexing and incubation in the dark for 30 min at room temperature. Afterwards, 20 µL of trypsin (50 ng μL^{-1}) solution that was prepared with 50 mM NH_4HCO_3 (pH 8.5) was added and the tubes placed in the thermomixer at 37 °C overnight. After that, 10 µL of trifluoroacetic acid (TFA) 5 % v/v was added to precipitate the surfactant *Rapi*GEST, the tubes were

vortexed and incubated at 37 °C for 90 min (without shaking), and centrifuged at 4000×*g* for 30 min at 4 °C. Then, 100 µL of the supernatant was collected and transferred to Total Recovery Vial (Waters, USA) for further shotgun mobility-DIA proteomics analysis.

Label-free protein quantification by MS

Qualitative and quantitative nano-ultra-high pressure chromatography (nanoUPLC) tandem nanoESI-HDMS^E (multiplexed DIA—data-independent acquisition) experiments were conducted using both a 1 h reverse-phase gradient from 7 to 40 % (v/v) acetonitrile (0.1 % v/v formic acid) and a 350 nL min^{-1} nanoACQUITY UPLC 2D Technology system. A nanoACQUITY UPLC HSS T3 1.8 µm, 75 µm × 150 mm column (pH 3) was used in conjunction with a reversed-phase (RP) XBridge BEH130 C_{18} 5 µm, 300 µm × 50 mm nanoflow column (pH 10).

For every measurement, the mass spectrometer was operated in resolution mode with a typical *m/z* resolving power of at least 35,000 FWHM and an ion mobility cell that was filled with nitrogen gas and a cross-section resolving power at least 40 Ω/ΔΩ. The effective resolution with the conjoined ion mobility was 1,800,000 FWHM. Analyses were performed using nano-electrospray ionization in positive ion mode nanoESI (+) and a NanoLockSpray (Waters, Manchester, UK) ionization source. The lock mass channel was sampled every 30 s. The mass spectrometer was calibrated with an MS/MS spectrum of [Glu1]-Fibrinopeptide B human (Glu-Fib) solution (100 fmol µL^{-1}) that was delivered through the reference sprayer of the NanoLockSpray source. $[M + 2H]^{2+} = 785.8426$) was used for initial single-point calibration, and MS/MS fragment ions of Glu-Fib were used to obtain the final instrument calibration.

DIA scanning with added specificity and selectivity of a non-linear 'T-wave' ion mobility (HDMS^E) device (Giles et al. 2011) was performed with a SYNAPT G2-Si HDMS mass spectrometer (Waters), which was automatically planned to switch between standard MS (3 eV) and elevated collision energies HDMS^E (19–45 eV) applied to the transfer 'T-wave' CID (collision-induced dissociation) cell with argon gas; the trap collision cell was adjusted to 1 eV, using a millisecond scan time that was previously adjusted based on the linear velocity of the chromatographic peak that was delivered through nanoACQUITY UPLC to generate a minimum of 20 scan points for each single peak, both in low-energy and high-energy transmission at an orthogonal acceleration time-of-flight (oa-TOF) and a mass range from *m/z* 50 to 2000. The RF offset (MS profile) was adjusted such that the nanoESI- HDMS^E data were effectively acquired from *m/z* 400 to 2000, ensuring that any masses that were observed in the high-energy spectra with less than m/z 400 arose from dissociations in the collision cell. The samples and conditions were injected with the same amount on the column. Stoichiometric measurements based on scouting runs of the integrated total ion account (TIC) prior to analysis were performed to ensure standardized molar values across all conditions.

Database searching and quantification

Progenesis QI for Proteomics Software V.2.0 (Nonlinear Dynamics, Newcastle, UK) was used to process the MS^E data. A protein databank from Pinidae subclass (Gymnosperm) was used, obtained from UniProt database (http://www.uniprot.org/taxonomy/3313).

The search conditions were based on taxonomy (Pinidae); maximum missed cleavages by trypsin allowed up to 1, variable modifications by carbamidomethyl (C) and acetyl N-terminal and oxidation (M); and a default maximum false discovery rate (FDR) value of 4 %. The obtained proteins were organized by software algorithm into a statistically significant list corresponding to increased and decreased regulation ratios between the different groups. Normalizations were performed automatically by Expression^E software, which was included inside PLGS informatics, using the recommended default parameters. Co-expressed proteins were filtered based on a fold change of $\log_2$ 1.2, as determined by the overall coefficient of variance for all quantified proteins across all replicates, and classified as up-regulated when $\log_2$ was 1.2 or greater and as down regulated when $\log_2$ was −1.2 or less.

For a functional context of the EC proteomics results, the identified proteins were further analyzed using Blast2GO, a bioinformatics tools for gene ontology (GO) based DNA or protein sequence annotation, to classify the biological process, cellular component, and molecular functional of the identified proteins (Götz et al. 2008).

Results

Global DNA methylation levels during long-term EC proliferation

Embryogenic cultures induced and maintained in PGR-free culture medium showed a heterogeneous pattern of GDM between successive multiplication cycles. Results indicated a significant increase in GDM levels in the first subculture cycle (20.04 %), followed by a decrease in the third cycle (15.38 %), equaling the levels found in zygotic embryos (15.98 %). In cycle 5 a decrease was observed, remaining constant in cycle 7, increasing (cycle 9) and decreasing

again (cycle 11). This unstable behavior persisted until the cycle 17 multiplication (Fig. 2A).

Differently, EC maintained in the PGR-supplemented culture medium showed a more regular pattern, with an initial significant reduction of the GDM in the cycle 1 (12.28 %) and 3 (10.62 %), then remaining stable until the cycle 7 (Fig. 2B). From the ninth cycle (12.96 %) there was a gradual and steady increase in GDM, resulting in 14.43 % at the cycle 17. The range of GDM variation in PGR-free treatment (10.55–20.04 %) was almost twice that observed in PGR-supplemented treatment (10.03–15.98 %).

Protein identification in PGR-free and -supplemented treatments

High-throughput proteomic screening identified 993 and 969 proteins for Cr01 and Cr02 cell lines, respectively. Among these, 293 and 283 (Cr01 and Cr02 cell lines, respectively) could be cross-referenced and annotated with the corresponding homolog protein in the accessed database. Thus, 29.36 % of the identified proteins could be annotated using sequence data from Pinidae subclass.

Differential expression analysis revealed 51 and 41 (Cr01 and Cr02 cell lines, respectively) up- or down-regulated proteins between the PGR-free and -supplemented treatment (see Supplementary Fig. S1 and S2). For EC subjected to PGR-supplemented treatment, 5 and 3 (Cr01 and Cr02 cell lines, respectively) unique proteins were identified and for EC from PGR-free treatment 2 unique proteins were found, from each cell line evaluated (Table 1).

Functional classification of proteins

Based on predicted biological process, most of the identified proteins in both cell lines and evaluated treatments were likely to be involved in metabolic, cellular and single-organism processes (Fig. 3a; see Supplementary Fig. S3A). Regarding the molecular function, the three top GO processes were catalytic activity, binding and structure molecule activity, also in both cell lines and evaluated treatments (Fig. 3b; see Supplementary Fig. S3B). For cellular component GO category, most of proteins were located in cell, organelle and macromolecular complex (Fig. 3c; see Supplementary Fig. S3C).

Regarding the differentially expressed proteins for Cr01 cell line in PGR-supplemented treatment, the three top GO processes for molecular function (level 3) were

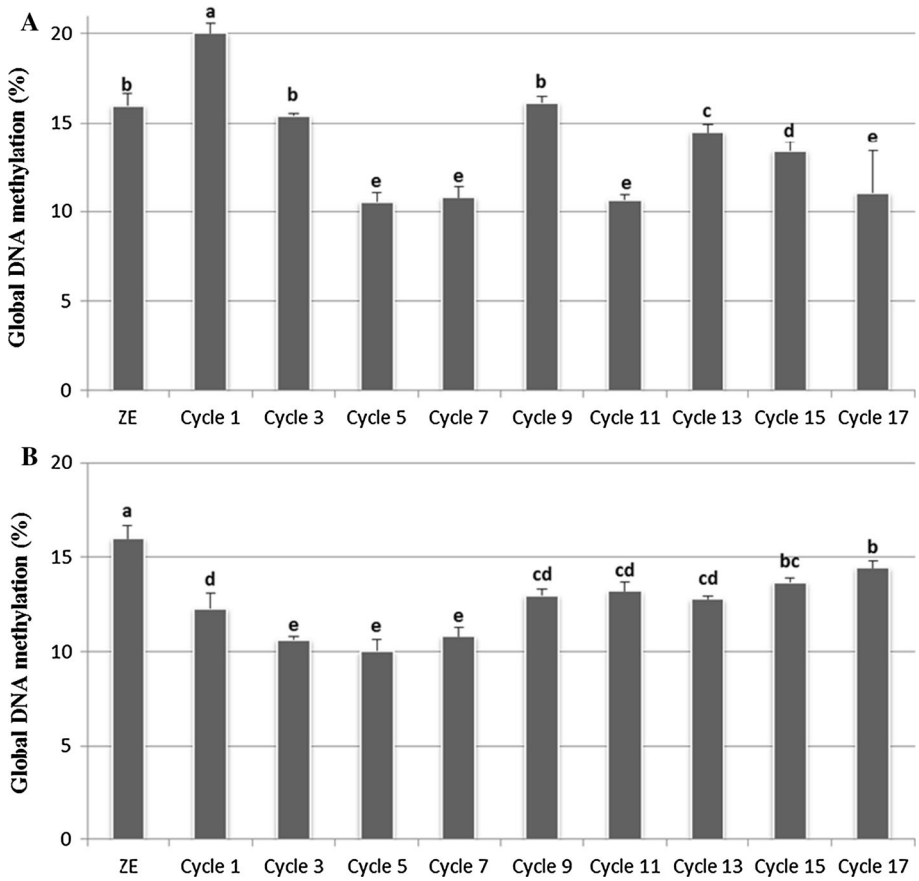

Fig. 2 Global DNA methylation levels after somatic embryogenesis induction (cycle 1) and during successive subculture cycles of *A. angustifolia* embryogenic cultures subjected to plant growth regulators-free (**A**) and -supplemented (**B**) treatments. Mean values followed by standard deviation (*vertical bars*). Means followed by lowercase *letters* are significantly different according to the SNK test ($p < 0.05$)

Table 1 Unique proteins identified in *A. angustifolia* embryogenic cultures from both cell lines (Cr01 and Cr02) subjected to plant growth regulators (PGR)-free or -supplemented treatments

Accession number	Description	Peptide count	Peptides used for quantitation
Unique proteins in PGR-supplemented treatment (Cr01)			
D0PPL9_9SPER	ATP synthase subunit alpha (Fragment)	16	1
C0PRH2_PICSI	Phosphoglycerate kinase	13	1
G8HSH5_9SPER	ATP synthase subunit alpha, chloroplastic	4	1
A9NZJ5_PICSI	Histone H2B	2	1
B8RIJ0_9SPER	Putative epoxide hydrolase (Fragment)	2	1
Unique proteins in PGR-free treatment (Cr01)			
B2KZJ2_PICAB	Putative senescence-associated protein (Fragment)	2	1
D5A831_PICSI	T-complex protein 1 subunit gamma	2	1
Unique proteins in PGR-supplemented treatment (Cr02)			
A0A075IEQ1_9SPER	PIN-like protein (Fragment)	4	1
A0A075E5K9_9SPER	DNA-directed RNA polymerase subunit alpha	3	1
C1IXS9_PINGE	DNA-directed RNA polymerase subunit beta	1	1
Unique proteins in PGR-free treatment (Cr02)			
B2KZJ2_PICAB	Putative senescence-associated protein (Fragment)	2	1
Q9BAN2_9SPER	Ribulose-1,5-bisphosphate carboxylase large subunit (Fragment)	9	1

"Peptide count" indicates number of peptides identified in this analysis

heterocyclic compound binding, organic cyclic compound binding and ion binding (Fig. 4a). These results were similar to that found in PGR-free treatment, which differ only in the third most common category, which was oxidoreductase activity (Fig. 4b). For Cr02 cell line the two top GO processes for molecular function were the same found in both treatments of Cr01 cell line (see Supplementary Fig. S4). The "transferase activity" and "ion binding" categories were the third most common in PGR-supplemented and –free treatments, respectively.

The most up-regulated protein for Cr01 cell line in PGR-supplemented treatment was E,E-α-farnesene synthase, categorized in "ion binding" molecular function and associated to terpene synthase activity, followed by Tau class glutathione S-transferase, categorized in "transferase activity" molecular function (Table 2). Many other proteins categorized in "transferase activity" were found up-regulated in this treatment, such as Zinc finger protein-related protein, Alpha-1,6-xylosyltransferase, RNA polymerase subunit and Gamma class glutathione S-transferase (Table 2). Another highlighted category found in this treatment was "structural constituent of ribosome", which was absent in PGR-free treatment (Fig. 4). Proteins associated to "oxidoreductase activity" were also up-regulated in this treatment, such as Cinnamyl alcohol dehydrogenase, Isoflavone reductase homolog 2, Isocitrate dehydrogenase [NAD] subunit, UDP-glucose 6-dehydrogenase and Thioredoxin reductase (Table 2).

The heat shock protein (70 kDa), assigned to "nucleotide binding" molecular function, and SKP1-interacting-like protein, assigned to "ligase activity" (Table 2) are among the most down-regulated proteins in PGR-supplemented treatment. One of the most abundant categories was the "oxidoreductase activity", corresponding to 40 % of annotated proteins, such as Malate dehydrogenase, Glyceraldehyde-3-phosphate dehydrogenase, Light-independent protochlorophyllide oxidoreductase subunitN, Probable cinnamyl alcohol dehydrogenase 7/8, Phosphoenolpyruvate carboxylase, Trans-cinnamate 4-hydroxylase 2 (Fig. 4b). An Auxin-responsive protein was also found down-regulated in PGR-supplemented treatment, assigned to "Response to endogenous stimulus" biological process (Table 2).

For Cr02 cell line, the most up-regulated protein in PGR-supplemented treatment was the histone H3, assigned to "DNA and protein binding" molecular function and related to cell cycle/DNA synthesis processes, followed by DNA-directed RNA polymerase, assigned to "DNA binding" and "Transferase activity", and Elongation factor 1-alpha, assigned to "Translation factor activity", "Binding" and "Transferase and Hidrolase activities" (Table 2). Similar to the results found in Cr01 cell line, one of the most representative categories was the "Transferase activity", with 35.71 % of annotated proteins, such as Lipoyl synthase, Zinc finger protein-related protein and Phytochrome (see Supplementary Fig. S4A). ABA and

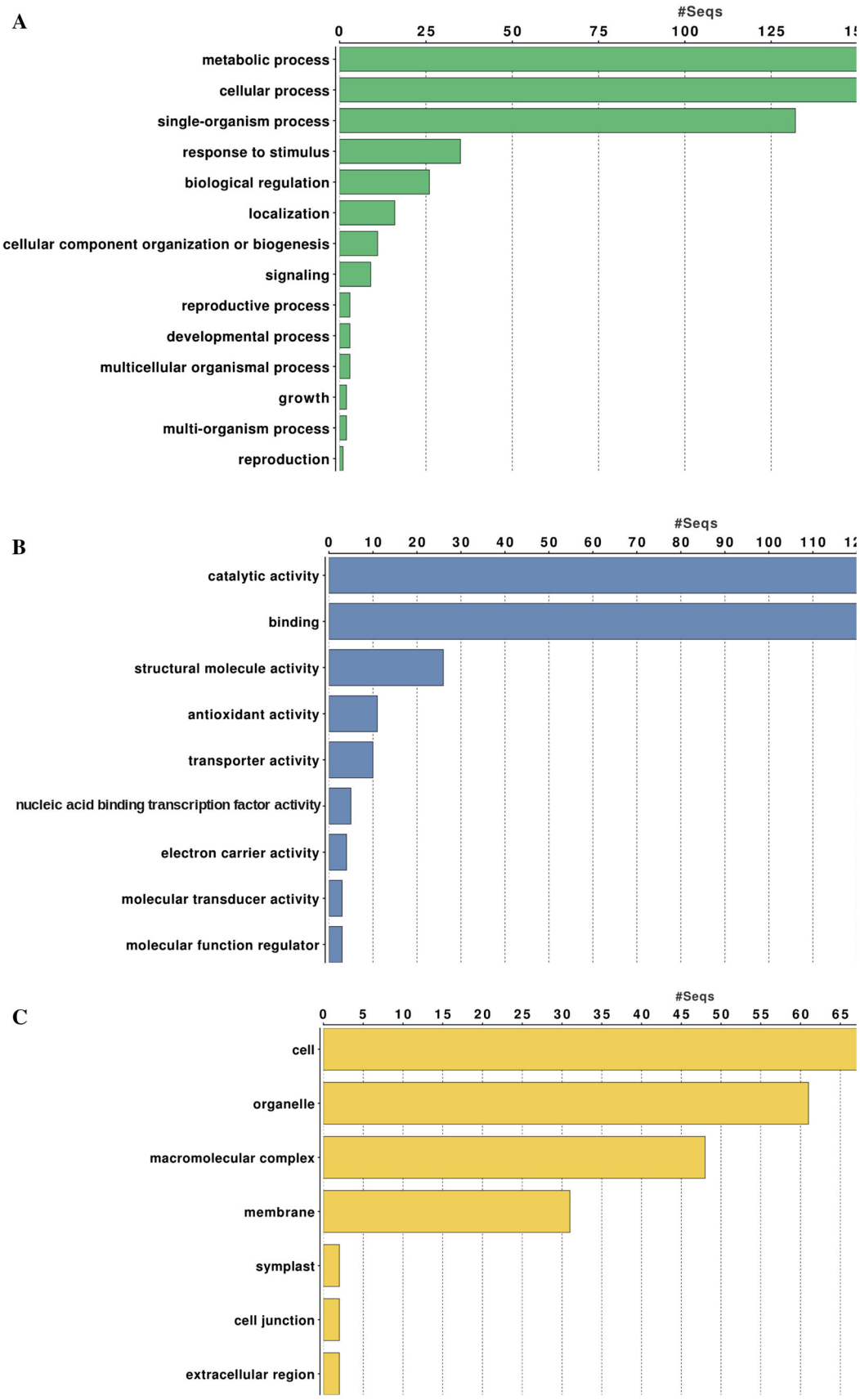
A
#Seqs
0 25 50 75 100 125
metabolic process
cellular process
single-organism process
response to stimulus
biological regulation
localization
cellular component organization or biogenesis
signaling
reproductive process
developmental process
multicellular organismal process
growth
multi-organism process
reproduction
B
#Seqs
0 10 20 30 40 50 60 70 80 90 100 110
catalytic activity
binding
structural molecule activity
antioxidant activity
transporter activity
nucleic acid binding transcription factor activity
electron carrier activity
molecular transducer activity
molecular function regulator
C
#Seqs
0 5 10 15 20 25 30 35 40 45 50 55 60 65
cell
organelle
macromolecular complex
membrane
symplast
cell junction
extracellular region

◀**Fig. 3** Functional classification of identified proteins in *A. angustifolia* embryogenic cultures from Cr01 cell line in both plant growth regulators treatments (supplemented or not) using Blast2GO software based on universal gene ontology (GO) annotation terms. The proteins were linked to at least one annotation term within the GO biological process (**a**), molecular function (**b**), and cellular component (**c**) categories. The histograms represent the number of proteins associated to level 2 GO categories

WDS induced 1 protein was also found up-regulated in this treatment, being assigned to "Response to stress" biological process (Table 2).

The most down-regulated protein found in PGR-supplemented treatment was the Actin 4, assigned to "Ion and small molecule binding" molecular function, followed by CYP720B1v2, assigned to "Catalytic activity" and

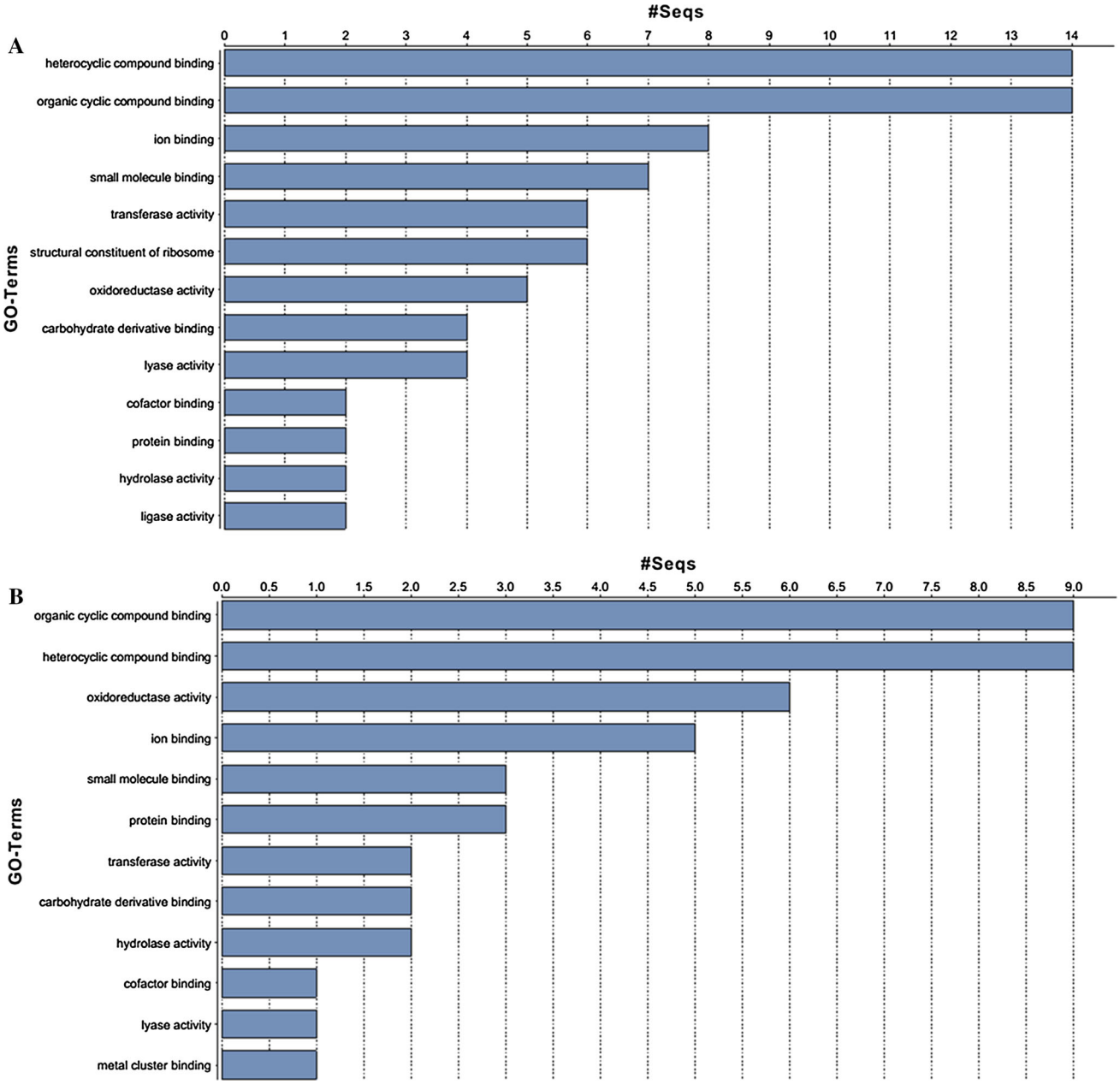

Fig. 4 Functional classification according to molecular function categories of differentially expressed proteins in *A. angustifolia* embryogenic cultures in both plant growth regulators treatments (supplemented or not) from Cr01 cell line using Blast2GO software based on universal gene ontology (GO) annotation terms. The histograms represent the number of proteins associated to level 3 GO categories

Table 2 Differentially expressed proteins identified in *A. angustifolia* embryogenic cultures from both cell lines (Cr01 and Cr02) subjected to plant growth regulators (PGR)-free or -supplemented treatments

Accession number	Description of homologous protein	Peptide count[a]	Ratio PGR-supplemented/-free[b]	Function[c]	Sub-cellular localization[d]
Up-regulated proteins in PGR-supplemented treatment (Cr01 cell line)					
Q675K8_PICAB	E,E-α-farnesene synthase	1	86.95	F: Catalytic activity, binding; P: Lipid metabolic process, Cellular process	Cytoplasm
L7S0Y4_PINTB	Tau class glutathione S-transferase	3	13.76	F: Transferase activity	Not assigned
B8LMY9_PICSI	Ubiquinone biosynthesis protein COQ4 homolog	1	9.25	P: Biosynthetic process, cellular process	Membrane; Mitochondria
Q0Q418_PINTA	Class III HD-Zip protein HDZ34 (Fragment)	1	8.50	F: DNA binding, Lipid binding	Nucleus
HSP02_PSEMZ	Putative heat shock protein 2 (Fragment)	1	7.44	Response to heat	Cytoplasm
I6Q476_9SPER	4-coumarate: coenzyme A ligase (Fragment)	4	7.04	F: Nucleotide binding, Catalytic activity; P: Secondary metabolic process, Cellular process	Not assigned
R9QW62_9SPER	Cinnamyl alcohol dehydrogenase (Fragment)	5	6.07	F: Catalytic activity, Binding; P: Secondary metabolic process, Biosynthetic process, Cellular process	Not assigned
B2KZF6_PICAB	Zinc finger protein-related protein (Fragment)	2	4.89	F: Transferase activity, binding; P: Cellular protein modification process	Not assigned
Q9MR99_TSUCA	ATP synthase subunit beta (Fragment)	10	4.77	F: Nucleotide binding, Transporter activity, Hidrolase activity; P: Biosynthetic process, Nucleobase-containing compound metabolic process	Membrane; Thylakoid; Plastid
G8J144_9SPER	30S ribosomal protein S2	1	4.22	F: Structural molecule activity; P: Translation	Plastid; Ribosome
G4LAW1_TAICR	30S ribosomal protein S3	2	4.16	F: RNA binding, Structural molecule activity; P: Translation	Plastid; Ribosome, Mitochondria
E6Y3C3_PINMO	WRKY transcription factor PmWRKY91 (Fragment)	1	4.09	F: DNA binding, Transcription factor activity, sequence specific DNA binding; P: Biosynthetic process, Nucleobase-containing compound metabolic process	Not assigned
Q9AVU0_PICAB	40S ribosomal protein S2	5	3.94	F: RNA binding, Structural molecule activity; P: Translation	Ribosome
A9NLS7_PICSI	60S ribosomal protein L6	3	3.84	F: Structural molecule activity; P: Translation	Ribosome
Q9FSD2_PINSY	Phytochrome (Fragment)	2	3.39	F: Protein binding, Receptor activity, Kinase activity, Signal transducer activity; P: Response to abiotic stimulus, Response to external stimulus, Cellular protein modification process, Biosynthetic process, Nucleobase-containing compound metabolic process	Intracellular; Membrane
TCTP_PSEMZ	Translationally-controlled tumor protein homolog	5	3.00	F: Protein binding; P: Embryo development,Signal transduction, Post-embryonic development, Anatomical structure morphogenesis, Pollination, Cell cycle, Response to stress, Response to abiotic stimulus, Response to endogenous stimulus, Cellular component organization, Cell differentiation, Cell growth	Golgi, Extracellular region; Vacuole; Plastid; Plasma membrane; Thylakoid; Nucleus; Intracellular

Table 2 continued

Accession number	Description of homologous protein	Peptide count[a]	Ratio PGR-supplemented/-free[b]	Function[c]	Sub-cellular localization[d]
Q6J0T7_PICGL	Type II CPD DNA photolyase (Fragment)	2	2.97	F: Nucleotide binding, DNA binding, Catalytic activity; P: Response to abiotic stimulus, DNA metabolic process, Response to stress	Nucleus
Q5TIN4_PINTA	Alpha-1,6-xylosyltransferase	1	2.94	F: Transferase activity	Golgi, Plasma membrane
Q29VH9_TAXWM	Taxadiene synthase	6	2.86	F: Catalytic activity, Binding; P: Lipid metabolic process, Biosynthetic process, Cellular process	Not assigned
Q5EKC1_PINTA	Phenylalanine ammonia-lyase 1 (Fragment)	1	2.78	F: Catalytic activity; P: Secondary metabolic process, Catabolic process, Biosynthetic process, Cellular process	Cytoplasm
B5T3M6_JUNVI	RNA polymerase subunit (Fragment)	1	2.72	F: DNA binding, Transferase activity; P: Biosynthetic process, Nucleobase-containing compound metabolic process	Plastid
V5W951_9SPER	Gamma class glutathione S-transferase	10	2.70	F: Translation factor activity, RNA binding, Transferase activity	Not assigned
R4L9Z6_CUNLA	Cytochrome c biogenesis protein CcsA	1	2.70	F: Binding; P: Cellular component organization	Membrane; Thylakoid; Plastid
IFRH2_PSEMZ	Isoflavone reductase homolog 2 (Fragments)	1	2.67	F: Catalytic activity	Cytoplasm
A9NVG2_PICSI	Isocitrate dehydrogenase [NAD] subunit	11	2.64	F: Nucleotide binding, Catalytic activity; P: Generation of precursor metabolites and energy	Mitochondria
L7RY37_9SPER	Rab GTPase (Fragment)	2	2.61	F: Nucleotide binding, Hidrolase activity; P: Signal transduction, Transport	Intracellular; Membrane
V5L1A8_9SPER	UDP-glucose 6-dehydrogenase	22	2.53	F: Nucleotide binding, Catalytic activity; P: Biosynthetic process, Nucleobase-containing compound metabolic process	Cytoplasm
A9NXV4_PICSI	Thioredoxin reductase	3	2.48	F: Catalytic activity,; P: Protein metabolic process, Cellular homeostasis, Post-embryonic development, Biosynthetic process, Pollination, Response to stress, Cell growth	Plastid; Cytoplasm; Mitochondria
A9NNS9_PICSI	Ribosomal protein	6	2.45	F: RNA binding, Structural molecule activity; P: Translation	Ribosome
B8LNN0_PICSI	40S ribosomal protein S12	2	2.38	F: Structural molecule activity; P: Translation	Ribosome
Down-regulated proteins in PGR-supplemented treatment (Cr01 cell line)					
C6FCI5_PSEMZ	Heat shock protein 70 kDa (Fragment)	11	0.42	F: Nucleotide binding	Not assigned
E0ZBJ0_PICSI	SKP1-interacting-like protein (Fragment)	2	0.41	F: Ligase activity; P: Biological process, Metabolic process	Not assigned
Q5DWG0_CRYJA	Thaumatin-like protein (Fragment)	1	0.40	Not assigned	Not assigned
A9NVT9_PICSI	Malate dehydrogenase	15	0.38	F: Catalytic activity; P: Carbohydrate metabolic process, Generation of precursor metabolites and energy	Cytoplasm

Table 2 continued

Accession number	Description of homologous protein	Peptide count[a]	Ratio PGR-supplemented/-free[b]	Function[c]	Sub-cellular localization[d]
G3PC_PINSY	Glyceraldehyde-3-phosphate dehydrogenase, cytosolic	16	0.36	F: Nucleotide binding, Catalytic activity; P: Carbohydrate metabolic process, Generation of precursor metabolites and energy, Catabolic process, Nucleobase-containing compound metabolic process	Cytoplasm
D5A7Y5_PICSI	Auxin-responsive protein	1	0.36	F: DNA binding; P: Signal transduction, Response to endogenous stimulus, Biosynthetic process, Nucleobase-containing compound metabolic process	Nucleus
A9NN85_PICSI	Small ubiquitin-related modifier	1	0.36	Not assigned	Nucleus
Q2L638_TAXDI	Light-independent protochlorophyllide oxidoreductase subunitN (Fragment)	1	0.36	F: Nucletide binding, Catalytic activity; P: Carbohydrate metabolic process, Photosynthesis, Biosynthetic process	Plastid
X2D433_JUNMO	Apocytochrome f	2	0.34	F: Binding; P: Photosynthesis	Membrane; Thylakoid; Plastid
D5AAB1_PICSI	Histone H2A	3	0.32	F: DNA binding, Protein binding	Nucleus
Q944N7_TAXWC	Paclitaxel/taxanoid biosynthesis susceptibility protein TS1 (Fragment)	1	0.28	F: Nucleic acid binding, Nuclease activity	Not assigned
CADH7_PICAB	Probable cinnamyl alcohol dehydrogenase 7/8	6	0.27	F: Catalytic activity, Binding; P: Secondary metabolic process, Biosynthetic process, Cellular process	Intracellular
Q711T3_PINPS	Histone H2A	4	0.21	F: DNA binding, Protein binding	Nucleus
G8IVK5_PINPU	ATP synthase subunit c, chloroplastic	1	0.19	F: Hidrogen ion transmembrane transporter activity, Lipid binding, Proton-transporting ATP synthase activity; P: Proton transport, Ion transport, Photosynthesis, Generation of precursor metabolites and energy, DNA-templated transcription, ATP byosynthetic process	Plastid; Tylakoid
Q9M3Y3_PINHA	Phosphoenolpyruvate carboxylase (Fragment)	3	0.16	F: Catalytic activity; P: Generation of precursor metabolites and energy, Photosynthesis	Cytoplasm
D2CNK0_PINBU	Maturase R (Fragment)	1	0.16	Not assigned	Mitochondria
A0A023W6Y7_PINPA	Trans-cinnamate 4-hydroxylase 2 (Fragment)	3	0.15	F: Protein binding, Catalytic activity; P: Secondary metabolic process, Multicellular organismal development, Biosynthetic process, Response to stress, Cellular process, Growth	Endoplasmic reticullum; Golgi; Vacuole; Plasma membrane; Cell wall
A9NUH0_PICSI	Endoglucanase	1	0.15	F: Hidrolase activity, Carbohydrate metabolic process, Catabolic process, Cellular process	Not assigned
O65863_PINEL	Reverse transcriptase (Fragment)	3	0.14	F: Transferase activity; P: Biosynthetic process, DNA metabolic process	Not assigned
G3C8Z9_PINPS	Phenylcoumaran benzylic ether reductase	5	0.05	Not assigned	Not assigned
Q8GUU4_PINPS	Chalcone synthase	4	0.04	F: Transferase activity; P: Biosynthetic process	Not assigned

Table 2 continued

Accession number	Description of homologous protein	Peptide count[a]	Ratio PGR-supplemented/-free[b]	Function[c]	Sub-cellular localization[d]
Up-regulated proteins in PGR-supplemented treatment (Cr02 cell line)					
K7NYB2_LARDC	Histone H3 (Fragment)	6	54.56	F: DNA binding, Protein binding; P: Carbohydrate metabolic process, Catabolic process, Transport	Nucleus
G8IUJ9_PINRI	DNA-directed RNA polymerase	7	34.06	F: DNA binding, Transferase activity; P: Biosynthetic process, Nucleobase-containing compound metabolic process	Plastid
R4IKK9_9SPER	Elongation factor 1-alpha	22	20.72	F: Nucleotide binding, Translation factor activity, RNA binding, Transferase activity, Hidrolase activity	Cytoplasm
Q9AVU0_PICAB	40S ribosomal protein S2	5	11.09	F: RNA binding, Structural molecule activity; P: Translation	Ribosome
A9NVN6_PICSI	Serine/threonine-protein phosphatase	1	8.66	F: Binding, Hidrolase activity; P: Cellular protein modification process	Cytoplasm
E0ZA86_PICSI	Leucine rich repeat-like protein (Fragment)	2	7.21	Not assigned	Not assigned
Q9XEW8_PICGL	14-3-3 protein	23	4.55	F: Protein binding	Not assigned
BAS1_PINST	Putative 2-Cys peroxiredoxin BAS1 (Fragments)	3	4.12	F: Catalytic activity	Plastid
R9QW62_9SPER	Cinnamyl alcohol dehydrogenase (Fragment)	5	4.04	F: Catalytic activity, Binding; P: Secondary metabolic process, Biosynthetic process, Cellular process	Not assigned
A9NZJ5_PICSI	Histone H2B	2	4.04	F: DNA binding, Protein binding	Nucleus
B2KZF6_PICAB	Zinc finger protein-related protein (Fragment)	2	3.85	F: Transferase activity, binding; P: Cellular protein modification process	Not assigned
Q9FSD2_PINSY	Phytochrome (Fragment)	2	2.68	F: Protein binding, Receptor activity, Kinase activity, Signal transducer activity; P: Response to abiotic stimulus, Response to external stimulus, Cellular protein modification process, Biosynthetic process, Nucleobase-containing compound metabolic process	Intracellular; Membrane
LIAS_PICSI	Lipoyl synthase	2	2.63	F: Binding, Transferase activity; P: Secondary metabolic process, Catabolic process, Multicellular organismal development, Lipid metabolic process, Cellular protein, modification process, Cell differentiation, Anatomical structure morphogenesis, Biosynthetic process, Nucleobase-containing compound metabolic process	Mitochondria
I3VMC1_PINMU	ABA and WDS induced 1 protein (Fragment)	1	2.49	P: Response to stress	Not assigned
E0ZCV6_PICSI	Basic endochitinase-like protein (Fragment)	1	2.41	F: Binding, Hidrolase activity; P: Carbohydrate metabolic process, Catabolic process, Cellular process	Not assigned

Table 2 continued

Accession number	Description of homologous protein	Peptide count[a]	Ratio PGR-supplemented/-free[b]	Function[c]	Sub-cellular localization[d]
C6FGA1_9SPER	Putative 60S ribosomal protein L10A (Fragment)	3	2.37	F: RNA binding, Structural molecule activity; P: Translation	Ribosome
Down-regulated proteins in PGR-supplemented treatment (Cr02 cell line)					
O24271_9SPER	Actin 4 (Fragment)	3	0.43	F: Nucleotide binding	Not assigned
A0A076U5K7_PINBN	CYP720B1v2	1	0.43	F: Catalytic activity, Binding	Membrane
B9VLC7_9SPER	AtpA	1	0.42	F: Nucleotide binding, Transporter activity, Hidrolase activity; P: Biosynthetic process, Nucleobase-containing compound metabolic process	Mitochondria; Membrane
Q9M520_TSUHE	Pinoresinol-lariciresinol reductase TH2	1	0.42	F: Catalytic activity; P: Secondary metabolic process, Catabolic process, Biosynthetic process, Cellular process	Not assigned
C4XUQ2_CRYJA	30S ribosomal protein S11	1	0.41	F: RNA binding, Structural molecule activity; P: Translation	Plastid; Ribosome
D5A8F9_PICSI	Succinyl-CoA ligase subunit beta	9	0.41	F:Nucleotide binding, Catalytic activity; P: Protein metabolic process, Carbohydrate metabolic process, Generation of precursor metabolites and energy, Response to abiotic stimulus, Catabolic process, Cellular component organization, Byosinthetic process, Nucleobase-containing compound metabolic process, Response to stress	Mitochondria
G8IU03_9SPER	Cytochrome b6-f complex subunit 6	1	0.41	F: Molecular function; P: Photosynthesis	Plastid; Thylakoid, Membrane
A0A097ZMV6_CRYJA	Putative PHYN2	1	0.40	F: Protein binding, Receptor activity, Kinase activity, Signal transducer activity; P: Response to abiotic stimulus, Response to external stimulus, Cellular protein modification process, Biosynthetic process, Nucleobase-containing compound metabolic proce	Membrane; Intracellular
B6V6Q0_9SPER	Putative carbonic anhydrase (Fragment)	3	0.37	F: Catalytic activity, Binding	Not assigned
C6F655_PSEMZ	Luminal binding protein (Fragment)	1	0.36	F: Nucleotide binding, Catalytic activity; P: Protein metabolic process, Response to abiotic stimulus, Cellular process, Response to stress	Endoplasmic reticullum
A0A068PCB8_9SPER	UDP-glucose pyrophosphorylase	5	0.35	F: Transferase activity; P: Nucleosome-containing compound metabolic process	Cytoplasm
E0ZBJ0_PICSI	SKP1-interacting-like protein (Fragment)	2	0.34	F: Ligase activity; P: Biological process, Metabolic process	Not assigned
O24270_9SPER	Actin 2 (Fragment)	2	0.34	F: Nucleotide binding	Not assigned
B1PID6_9SPER	Putative chaperonin family protein	2	0.32	F: Nucleotide binding, Protein binding; P: Protein metabolic process, Cellular process	Cytoplasm

Table 2 continued

Accession number	Description of homologous protein	Peptide count[a]	Ratio PGR-supplemented/-free[b]	Function[c]	Sub-cellular localization[d]
C0PS33_PICSI	mRNA cap guanine-N7 methyltransferase	1	0.32	F: RNA binding, Transferase activity; P: Nucleobase-containing compound metabolic process	Nucleus
CADH7_PICAB	Probable cinnamyl alcohol dehydrogenase 7/8	1	0.25	F: Catalytic activity, Binding; P: Secondary metabolic process, Biosynthetic process, Cellular process	Intracellular
B0ZR82_PINRA	Catechol O-methyltransferase (Fragment)	1	0.25	F: Transferase activity	Not assigned
A9NUH1_PICSI	N-acetyl-gamma-glutamyl-phosphate reductase	1	0.20	F: Nucleotide binding, Protein binding, Catalytic activity; P: Flower development, Biosynthetic process, Cellular process	Membrane; Nucleolus; Plastid
A9NUH0_PICSI	Endoglucanase	1	0.19	F: Hidrolase activity, Carbohydrate metabolic process, Catabolic process, Cellular process	Not assigned
C3VYB7_9SPER	DNA-directed RNA polymerase subunit alpha	3	0.18	F: DNA binding, Protein binding, Transferase activity; P: Biosynthetic process, DNA metabolic process, Response to stress	Plastid
Q1XG58_CRYJA	Putative elongation factor	1	0.13	F: Translation factor activity, RNA binding; P: Secondary metabolic process, Catabolic process	Cytoplasm; Golgi; Plasma membrane
A9NMW7_PICSI	Thioredoxin	1	0.12	F: Catalytic activity; P: Cellular homeostasis, Cell communication	Nucleus; Cytosol; Plastid
Q5DWG0_CRYJA	Thaumatin-like protein (Fragment)	1	0.10	Not assigned	Not assigned
A9NZ28_PICSI	Ribosomal protein L15	1	0.09	F: Structural molecule activity; P: Translation	Ribosome
Q944N7_TAXWC	Paclitaxel/taxanoid biosynthesis susceptibility protein TS1 (Fragment)	1	0.08	F: Nucleic acid binding, Nuclease activity	Not assigned

[a] "Peptide count" indicates number of peptides identified in this analysis

[b] "Ratio PGR-supplemented/-free" indicates the differential protein expression ratio between embryogenic cultures subjected to plant growth regulators (PGR)–supplemented compared to -free treatment

[c] "Function" indicates protein function according to its molecular function (F) and/or biological process (P) categorized using Blast2GO results

[d] "Sub-cellular localization" indicates protein localization predicted by Blast2GO results

"Binding" (Table 2). The categories "Carbohydrate derivative binding" and "Oxidoreductase activity" were notably more representative than that observed in up-regulated proteins in this cell line, with three times more proteins present in these categories (see Supplementary Fig. S4).

Between five unique proteins expressed in PGR-supplemented treatment (Cr01 cell line), two were assigned for ATP synthesis, one for glycolytic process, one for hydrolase activity and the last one for DNA-binding (Table 1). Unique proteins for Cr02 cell line in PGR-supplemented treatment were different, with two DNA-directed RNA polymerase, associated in the transcription process, and the interesting PIN-like protein, known for its involvement in polar auxin transport. Unique proteins found in PGR-free treatment showed one protein in common for both cell lines, the putative senescence-associated protein, involved in the translation process, and a uniquely expressed protein in each cell line, which were related to protein folding (Cr01 cell line) and carbon fixation (Cr02 cell line).

Discussion

Global DNA methylation is affected by PGRs supplementation during successive EC subcultures

During 1 year subcultures, GDM could be monitored and contrasted with the initial explant levels. The results of GDM for EC induced and maintained in PGR-free or -supplemented treatments indicated, as expected, distinct behaviors.

Results indicated a differentiated initial response (cycle 1) of EC from PGR-free treatment, showing a significant increase in GDM levels, the opposite situation (significant decrease) was observed in PGR-supplemented treatment (Fig. 2). Dedifferentiation process occurred during SE induction is a key-step to obtaining EC. This process is thought to be achieved through the erasing of some, if not all, of the pre-existing epigenetic marks (and among them, DNA methylation) across the genome (Feng et al. 2010; Jacob and Martienssen 2011; Rival et al. 2013). Our results showed that, in fact, GDM differed from the initial status (zygotic embryo); however, contrasting responses were observed for EC from PGR-free or -supplemented treatments.

Several studies have suggested the existence of a progressive DNA methylation along with plant development, in a similar way to that described throughout mammals embryonic development (Goto and Monk 1998; Hsieh 2000; Ruiz-García et al. 2005). Teyssier et al. (2014) suggested that global DNA hypermethylation in EC is associated with somatic embryos differentiation in hybrid larch (*Larix* × *eurolepis*). In our results, increased GDM in the induced EC on PGR-free culture medium may indicate that, despite the occurrence of the dedifferentiation process in most cells, a portion of these cells may have committed to the beginning of embryonic development process, causing an increase in GDM levels. On the other extreme, the significant decrease in GDM after EC induction on PGR-supplemented treatment may suggest a more uniform pattern in cell dedifferentiation and maintenance of the cells in an undifferentiated state.

Subsequent subculture cycles of EC in PGR-free treatment maintained an oscillating GDM pattern, but without achieving the highest values found after the first subculture. For EC maintained in PGR-supplemented culture medium GDM gradually increased, until cycle 17 of subcultures. Although no other studies comparing the GDM of EC maintained in PGR presence or absence, the consequences of long-term in vitro propagation on GDM levels of cultured plant cells have been the subject of several recent investigations.

Taxus media and *Elaeis guineensis* cell cultures during long-term propagation showed a time-dependent GDM increase quantified by HPLC, whereas for *T. media* MSAP (methylation sensitive amplification polymorphism) analyses revealed a number of locus-specific methylation gains and losses throughout the period (Fu et al. 2012; Rival et al. 2013). The same authors stated that GDM could be modulated by the environmental conditions imposed on in vitro cultivated cells, with a long series of subcultures inducing a sizeable increase in GDM. Our results for EC derived from PGR-supplemented treatment corroborate this idea, with increased GDM during prolonged subcultures; however, the same is not true for EC maintained on PGR-free treatment, highlighting the possible PGR role in this process.

Correlations between GDM levels and morphogenetic response have previously been reported for several plant species (Lambé et al. 1997; Fraga et al. 2002; Noceda et al. 2009; Klimaszewska et al. 2009; Fraga et al. 2012; Rival et al. 2013; Teyssier et al. 2014). Many angiosperm species show variations in GDM during SE, with embryogenic cell lines generally exhibiting lower GDM levels than non-embryogenic lines (LoSchiavo et al. 1989; Miguel and Marum 2011). In gymnosperms, Noceda et al. (2009) also reported a clear negative correlation between GDM level and embryogenic competence in *Pinus nigra* EC.

In the present study, we do not present results associated with morphogenetic response of EC from PGR-free or -supplemented treatments subjected to the maturation step; however, a recent study published by our research group reported promising results with EC from the same cell line evaluated in this study (Cr01) induced and maintained in PGR-free culture medium (Fraga et al. 2015). Differently,

preliminary assays performed in our laboratory with EC derived from PGR-supplemented treatment demonstrated poor responsiveness to maturation treatment (data not shown).

The use of synthetic auxin analogues, such as 2,4-D, used in PGR-supplemented treatment in the present study, have been frequently linked to compromise genomic stability through the promotion of DNA methylation deregulation coupled with gene expression modifications (LoSchiavo et al. 1989; Bairu et al. 2006; Krogan and Long 2009). A recent report by Zhang et al. (2012) provides evidence of a functional interplay between environmentally induced epigenetic modifications, response to PGRs and phenotypic plasticity. Our results showed that PGR-supplementation affects GDM in a long-term maintained EC; nonetheless, more evidence is necessary to demonstrate a possible deregulatory effect on embryogenic competence of those EC.

Label-free proteomic analysis

Here, we describe for the first time in this species a label-free proteomic approach, using 2D-nanoESI-HDMS^E technology, which proved to be a reliable alternative for large-scale protein identification in *A. angustifolia* EC. According to the protein functional classification, most of the identified proteins were likely to be involved in metabolic, cellular and single-organism processes, for biological process GO category; catalytic activity, binding and structure molecule activity, for molecular function; and located in cell, organelle and macromolecular complex, for cellular component GO category. These results corroborate the functional annotation of the embryogenesis reference transcriptome for this species (Elbl et al. 2015), where the most highly represented GO categories were almost the same found in our results, indicating consistency in proteomic data obtained in our study.

PIN-like protein is exclusively expressed in PGR-supplemented treatment

Auxin is a central regulator in many processes during plant growth and development, and is mainly directional transported through the plant (Friml et al. 2003). This polar auxin transport (PAT) is important for many auxin-regulated processes and requires the activity of polarly localized efflux regulators, represented by members of the PIN-FORMED family (Weijers et al. 2005). The PIN-FORMED (PIN) proteins are a plant-specific family of transmembrane proteins that transport the plant signal molecule (phytohormone) auxin as their substrate (Křeček et al. 2009). In land plants, the PIN proteins act as key regulators in multiple developmental events ranging from embryogenesis through morphogenesis and organogenesis to growth responses to environmental stimuli (Křeček et al. 2009). Here, we describe for the first time in a proteomic study the PIN-like protein expression during somatic embryogenesis (Table 1). This protein was exclusively expressed in EC from Cr02 cell line subjected to PGR-supplemented treatment.

Auxin itself upregulates the transcription of PINs, and other phytohormones and PGRs also influence the activity of the PIN promoters to various degrees; however, the effects are organ- or even cell-type-specific and strongly depend on the particular part of the plant examined and PGR used (Křeček et al. 2009). Not surprisingly, PIN-like protein was found as unique expressed protein in PGR-supplemented treatment in our results. Nevertheless, the specific effect of this protein expression in EC subjected to PGR-supplementation and its consequences in the maturation step remain unclear.

Recently, Elbl et al. (2015), based on transcriptome data of *A. angustifolia* SE, suggested that early somatic embryos fails to establish the correct auxin distribution due to *WUSCHEL* over-expression, which may be culminates in altered polar auxin flux. In that study, the authors used another culture medium composition, plant genotype and PGR-free treatment, culture conditions quite distinct from those used in this study.

Differentially expressed proteins in PGR-free and -supplemented treatments are related to terpenoid biosynthesis

E,E-α-farnesene synthase were the most up-regulated protein detected in EC induced and maintained in PGR-supplemented treatment, from Cr01 cell line (Table 2). This enzyme converts farnesyl diphosphate (FDP) to (E,E)-α-farnesene, a sesquiterpene hydrocarbon produced by many plant species in a range of tissues, in response to pathogens (Huang et al. 2003), or on wounding by herbivores (Vuorinen et al. 2004). To date, there are no reports on up-regulation of this protein in plant SE.

There is evidence that expression of the gene encoding α-farnesene synthase is induced by ethylene (Gapper et al. 2006). Jo et al. (2013) reported improved ethylene levels in *A. angustifolia* EC responsive to maturation from PGR-free culture medium during proliferation. In another report involving modulation of ethylene levels, an increased synthesis was observed in response to application of high amounts of 2,4-D, which impaired embryo development (Minocha and Minocha 1995). In our results, the up-regulation of E,E-α-farnesene synthase may be related to ethylene synthesis and, consequently, PGR supplementation.

Surprisingly, another up-regulated protein found in PGR-supplemented treatment was taxadiene synthase.

Taxadiene synthase is a key enzyme catalyzing the first committed step of the biosynthetic pathway of Taxol™ (paclitaxel), a diterpenoid that can be found in the bark and needles of different species of *Taxus* (Khan et al. 2009).

Other strong evidence for enhanced terpenoid synthesis in these *A. angustifolia* EC is the phenylalanine ammonia-lyase 1 (PAL) up-regulation (Table 2). PAL substrate, phenylalanine, is an important precursor for the side chain and the C2 benzoyl group (Brincat et al. 2002). In addition, the use of cinnamic acid and other PAL inhibitors in order to increase the availability of phenylalanine might result in enhanced Taxol production. Once again, up-regulation of this protein may be related to the Taxol production in these EC; however, further studies quantifying the Taxol levels can confirm whether or not this hypothesis.

Stress-related proteins are differentially expressed between PGR-free and -supplemented treatments

Another interesting up-regulated protein detected in PGR-supplemented EC was Tau class glutathione S-transferase. Glutathione-S-transferases (GSTs) are the enzymes that catalyze the conjugation of the tripeptide glutathione (GSH) to a wide variety of hydrophobic, electrophilic, and cytotoxic substrates. Many GSTs also act as GSH-dependent peroxidases by catalyzing the reduction of organic hydroperoxide to the less toxic monohydroxy alcohols (Gong et al. 2005). Plant GSTs have been intensively studied for their ability to detoxify herbicides (Flocco et al. 2004). Members of the GST gene family are upregulated during auxin-induced SE, and GST induction is auxin regulated (Marsoni et al. 2008). This enzyme catalyzes GSH conjugation to herbicide molecules, to form glutathione-S-conjugates, which are then imported to vacuoles, thus protecting the plants from damage by herbicides (Gong et al. 2005). So, in general, plants with higher GST levels are more tolerant to herbicide exposure. The PGR supplementation evaluated in this study mainly contains 2,4-D, an auxin analog herbicide. Thus, the high expression level of this enzyme on EC subjected to PGR-supplemented treatment is apparently related to improved capability of herbicide detoxification via GSH conjugation by activation of GST activity.

Other stress-related proteins were also up-regulated in PGR-supplemented treatment (Table 2). Oxidative stress caused by increased levels of radical oxygen species (ROS) has been reported to enhance SE in many plant species (Caliskan et al. 2004). ROS has been implicated also as a second messenger during auxin and stress-induced embryogenesis, and maybe act as signaling molecules playing an important role during auxin induced SE (Marsoni et al. 2008). Thus, the improved expression of these proteins in EC subjected to PGR-supplemented treatment maybe also associated to auxin stress responses.

Between stress-related proteins up-regulated in PGR-supplemented treatment, special attention should be paid to ABA and WDS induced 1 protein (Table 2). The ABA and water-deficit stress (WDS)-induced proteins represent a family of plant proteins induced by WDS or ABA stress and ripening (Sang et al. 2012). The role of these proteins at the molecular level is unclear, but they have been observed to be up-regulated in a number of plant species as a consequence of WDS (Padmanabhan et al. 1997).

The up-regulation of ABA and WDS induced 1 protein found in the present study may also indicate that these EC can contain high endogenous ABA levels, compared to EC maintained in PGR-free culture medium. According to Stasolla and Yeung (2003), the endogenous ABA levels in gymnosperms are normally low during the initial phases of embryonic development, and higher levels were associated with developmental failure. Farias-Soares et al. (2014) reported that the decrease in ABA levels was coincident with an increase in the frequency of pro-embryos formation in *A. angustifolia*. Based on this notion, PGR supplementation may be causing WDS on *A. angustifolia* EC, possibly related to undesirable improved ABA levels.

A pathogenesis-related thaumatin-like protein was up-regulated in PGR-free treatment, in both cell lines evaluated. This protein accumulates in response to stress, such as wounding, infection by a virus or fungus, and osmotic stress (Yasuda et al. 2001). Their synthesis during in vitro conditions could be related with the adaptation of the plant cells to new environmental conditions, which, in a first phase, may be perceived by the cells as unfavorable, hence resulting in the activation of defense mechanisms probably not directly related with a specific morphogenetic pathway, such as SE (Correia et al. 2012). The same authors hypothesized that, alternatively, the stress response of plant cells may activate signaling pathways, triggering cellular events leading to the formation of embryonary structures. Our evidences that EC derived from PGR-free treatment have improved responses to maturation treatment may be in accordance to this hypothesis.

Proteins involved in protein folding and stabilization appear to be enhanced in PGR-free treatment

The most down-regulated protein in PGR-supplemented treatment for Cr01 cell line was assigned to the family of 70 kDa heat shock proteins (Hsp70 s). The Hsp70 s act as molecular chaperones and play essential roles in protein biogenesis, transport and degradation (Morano et al. 2012). Their function may be of increased importance under stress conditions, where misfolding of polypeptides occurs more commonly (Zhang et al. 2009). In addition, Hsp70 s have

been associated to normal development during embryogenesis and seed germination (Waters et al. 2008). Furthermore, these proteins play a role in translocation of proteins across membranes by maintaining proteins in an extended translocation-competent conformation that also affects reserve mobilization (Latijnhouwers et al. 2010).

Members of the heat shock protein family have been reported to be highly expressed during initiation of SE from somatic cells, microspores and developing pollen in alfalfa and tobacco and from hypocotyls in carrots (Györgyey et al. 1991; Zarsky et al. 1995; Kitamya et al. 2000). Marsoni et al. (2008) also found Hsp70 s up-regulated during *Vitis vinifera* SE. Fraga et al. (2013) reported the presence of these proteins in the normal somatic plantlets and its absence in the off-types plantlets derived from somatic embryos of *Acca sellowiana*.

In the same way, luminal binding protein, also a member of the Hsp70 s, was up-regulated in PGR-free treatment for Cr02 cell line (Table 2). In Douglas fir, this protein was shown to be regulated during seed development and early seedling growth (Forward and Misra 2000). On the contrary, Teyssier et al. (2014) reported that Hsps were present in higher levels at the late embryogenesis stage than at the early stage, probably in order to prepare the embryos for desiccation. Thus, the up-regulation of Hsp70 s in PGR-free treatment could also play a protective function in response to the stress conditions that characterize in vitro growth, and provide an adaptive advantage to these EC.

Putative chaperonin family protein was also up-regulated in PGR-free treatment (Cr02 cell line). Chaperones are overexpressed under several types of stress in in vitro conditions (Correia et al. 2012). These proteins are also known for their roles in the maturation of protein complexes and in facilitating the folding process of newly synthesized proteins, similarly to above described proteins from Hsp70 s family.

Concluding remarks

Our approach to investigate the effect of PGR-free and -supplemented treatments in *A. angustifolia* EC allowed the identification of different scenarios between them in an unprecedented way.

GDM differed from the initial status (zygotic embryo) in both treatments, and diverse responses were observed between EC from PGR-free and -supplemented treatments. Increased GDM in EC induced on PGR-free culture medium may indicate that, despite the occurrence of the dedifferentiation process in most cells, a portion of these cells may have committed to the beginning of embryonic development process, causing an increase in GDM levels. Otherwise, the significant decrease in GDM after EC induction on PGR-supplemented treatment may indicate a more uniform pattern in cell dedifferentiation and maintenance of the cells in an undifferentiated state. During long-term subcultures, PGR-supplementation proved to gradually increase the GDM levels, which has frequently been linked to compromise genomic stability and evoke gene expression modifications.

Label-free proteomics proved to be a reliable method for large-scale protein identification in *A. angustifolia* EC, enabling a robust protein identification and quantification. Exclusively expression of PIN-like protein in PGR-supplemented treatment indicated a possible differential response of the EC to polar auxin transport, which can generate implications in its morphogenetic response to maturation step. Regarding to differentially expressed proteins, up-regulation of stress-related proteins in EC from PGR-supplemented treatment, such as GSTs, suggests a more stressful environment, triggering notable responses to hormonal, osmotic and oxidative stresses. In the same way, improved expression of proteins involved with protein folding and stabilization processes in PGR-free treatment, such as Hsps, could play a protective function in response to the stress conditions caused by in vitro culture, and may provide an adaptive advantage to these EC. The expression of several proteins associated to terpenoid biosynthesis pathways suggests that EC from both evaluated treatments and cell lines possibly are producing these compounds, may be a first report for a conifer species that does not belong to *Taxus* genus.

Acknowledgments This work was supported by Coordenação de Aperfeiçoamento de Pessoal de Nível Superior (CAPES), Conselho Nacional de Desenvolvimento Científico e Tecnológico (CNPq 478393/2013-0, and 306126/2013-3), and Fundação de Amparo à Pesquisa e Inovação do Estado de Santa Catarina (FAPESC 14848/2011-2, 3770/2012, and 2780/2012-4). The authors are also grateful to the Unidade de Biologia Integrativa (BioInt) of Universidade Estadual do Norte Fluminense Darcy Ribeiro (UENF) for the support in the shotgun proteomics analysis.

Author contribution statement Conceived and designed the experiments: HPFF, LNV and MPG; Performed the in vitro culture experiments and DNA methylation analysis: HPFF, LNV and CCP; Performed the label-free proteomics and data analysis: HPFF, ASH and VS; Contributed reagents/materials/analysis tools: VS and MPG; Wrote the paper: HPFF, LNV and MPG.

References

Abril N, Gion JM, Kerner R, Müller-Starck G, Cerrillo RMN, Plomion C et al (2011) Proteomics research on forest trees, the most recalcitrant and orphan plant species. Phytochemistry 72:1219–1242

Bairu MW, Fennell CW, van Staden J (2006) The effect of plant growth regulators on somaclonal variation in Cavendish banana (*Musa* AAA cv. ''Zelig''). Sci Hortic 108:347–351

Balbuena TS, Silveira V, Junqueira M, Dias LL, Santa-Catarina C, Shevchenko A et al (2009) Changes in the 2-DE protein profile during zygotic embryogenesis in the Brazilian Pine (*Araucaria angustifolia*). J Proteomics 72:337–352

Balbuena TS, Jo L, Pieruzzi FP, Dias LL, Silveira V, Santa-Catarina C et al (2011) Differential proteome analysis of mature and germinated embryos of *Araucaria angustifolia*. Phytochemistry 72:302–311

Brincat MC, Gibson DM, Shuler ML (2002) Alterations in taxol production in plant cell culture via manipulation of the phenylalanine ammonia lyase pathway. Biotechnol Prog 18:1149–1156

Caliskan M, Turet M, Cuming AC (2004) Formation of wheat (*Triticum aestivum* L.) embryogenic callus involves peroxide-generating germin-like oxalate oxidase. Planta 219:132–140

Cangahuala-Inocente GC, Villarino A, Seixas D, Dumas-Gaudot E, Terenzi H, Guerra MP (2009) Differential proteomic analysis of developmental stages of *Acca sellowiana* somatic embryos. Acta Physiol Plant 31:501–514

Carpentier SC, Panis B, Vertommen A, Swennen R, Sergeant K, Renaut J et al (2008) Proteome analysis of non-model plants: a challenging but powerful approach. Mass Spectrom Rev 27:354–377

Chen S, Harmon AC (2006) Advances in plant proteomics. Proteomics 6:5504–5516

Chen EI, Hewel J, Felding-Habermann B, Yates JR (2006) Large scale protein profiling by combination of protein fractionation and multidimensional protein identification technology (Mud-PIT). Mol Cell Proteomics 5:53–56

Correia S, Vinhas R, Manadas B, Lourenço AS, Veríssimo P, Canhoto JM (2012) Comparative proteomic analysis of auxin-induced embryogenic and nonembryogenic tissues of the solanaceous tree *Cyphomandra betacea* (Tamarillo). J Proteome Res 11:1666–1675

Doyle JJ (1987) A rapid DNA isolation procedure for small quantities of fresh leaf tissue. Phytochem Bull 19:11–15

Elbl P, Lira BS, Andrade SCS, Jo L, dos Santos ALW, Coutinho LL et al (2015) Comparative transcriptome analysis of early somatic embryo formation and seed development in Brazilian pine, *Araucaria angustifolia* (Bertol.) Kuntze. Plant Cell Tiss Org Cult 120:903–915

Farias-Soares FL, Steiner N, Schmidt EC, Pereira MLT, Rogge-Renner GD, Bouzon ZL et al (2014) The transition of proembryogenic masses to somatic embryos in *Araucaria angustifolia* (Bertol.) Kuntze is related to the endogenous contents of IAA, ABA and polyamines. Acta Physiol Plant 36:1853–1865

Feng S, Jacobsen SE, Reik W (2010) Epigenetic reprogramming in plant and animal development. Science 330:622–627

Flocco CG, Lindblom SD, Elizabeth AH, Smits P (2004) Overexpression of enzymes involved in glutathione synthesis enhances tolerance to organic pollutants in *Brassica juncea*. Int J Phytoremediat 6:289–304

Forward BS, Misra S (2000) Characterization and expression of the Douglas-fir luminal binding protein (PmBiP). Planta 212:41–51

Fraga MF, Rodríguez R, Cañal MJ (2002) Genomic DNA methylation-demethylation during aging and reinvigoration of *Pinus radiata*. Tree Physiol 22:813–816

Fraga HPF, Vieira LN, Caprestano CA, Steinmacher DA, Micke GA, Spudeit DA et al (2012) 5-Azacytidine combined with 2,4-D improves somatic embryogenesis of *Acca sellowiana* (O. Berg) Burret by means of changes in global DNA methylation levels. Plant Cell Rep 31:2165–2176

Fraga HPF, Agapito-Tenfen SZ, Caprestano CA, Nodari RO, Guerra MP (2013) Comparative proteomic analysis of off-type and normal phenotype somatic plantlets derived from somatic embryos of Feijoa (*Acca sellowiana* (O. Berg) Burret). Plant Sci 210:224–231

Fraga HPF, Vieira LN, Puttkammer CC, Oliveira EM, Guerra MP (2015) Time-lapse cell tracking reveals morphohistological features in somatic embryogenesis of *Araucaria angustifolia* (Bert) O. Kuntze. Trees. doi:10.1007/s00468-015-1244-x

Friml J, Vieten A, Sauer M, Weijers D, Schwarz H, Hamann T et al (2003) Efflux-dependent auxin gradients establish the apical–basal axis of *Arabidopsis*. Nature 426:147–153

Fu C, Li L, Wu W, Li M, Yu X, Yu L (2012) Assessment of genetic and epigenetic variation during long-term *Taxus* cell culture. Plant Cell Rep 31:1321–1331

Gapper NE, Bai J, Whitaker BD (2006) Inhibition of ethylene-induced α-farnesene synthase gene PcAFS1 expression in 'd'Anjou' pears with 1-MCP reduces synthesis and oxidation of α-farnesene and delays development of superficial scald. Postharvest Biol Technol 41:225–233

Geromanos SJ, Vissers JP, Silva JC, Dorschel CA, Li GZ, Gorenstein MV et al (2009) The detection, correlation, and comparison of peptide precursor and product ions from data independent LC-MS with data dependent LC-MS/MS. Proteomics 9:1683–1695

Giles K, Williams JP, Campuzano I (2011) Enhancements in travelling wave ion mobility resolution. Rapid Commun Mass Spectrom 25:1559–1566

Gong H, Jiao Y, Hu WW, Pua EC (2005) Expression of glutathione-S-transferase and its role in plant growth and development in vivo and shoot morphogenesis in vitro. Plant Mol Biol 57:53–66

Goto T, Monk M (1998) Regulation of X-chromosome inactivation in development in mice and humans. Microbiol Mol Biol Rev 62:362–378

Götz S, García-Gómez JM, Terol J, Williams TD, Nagaraj SH, Nueda MJ et al (2008) High-throughput functional annotation and data mining with the Blast2GO suite. Nucleic Acids Res 36:3420–3435

Guerra MP, Silveira V, dos Santos ALW, Astarita LV, Nodari RO (2000) Somatic embryogenesis in *Araucaria angustifolia* (Bert) O. Ktze. In: Jain SM, Gupta PK, Newton RJ (eds) Somatic embryogenesis in woody plants. Kluwer Academic Publishers, Dordrecht, pp 457–478

Guerra MP, Steiner N, Mantovani A, Nodari RO, Reis MS, dos Santos KL (2008) Evolução, ontogênese e diversidade genética em *Araucaria angustifolia*. In: Barbieri RL, Stumpf ERT (eds) Origem e evolução de plantas cultivadas. Embrapa Informação Tecnológica, Brasilia, pp 149–184

Gupta PK, Pullman G (1991) Method for reproducing coniferous plants by somatic embryogenesis using abscisic acid and osmotic potential variation. U.S. Patent No. 5,036,007

Györgyey J, Gartner A, Németh K, Magyar Z, Hirt H, Heberle-Bors E et al (1991) Alfalfa heat shock genes are differentially expressed during somatic embryogenesis. Plant Mol Biol 16:999–1007

Heringer AS, Chiquieri TB, Macedo AF, Santa-Catarina C, Souza GHMF, Floh EIS et al (2015) Label-free quantitative proteomics of embryogenic and non-embryogenic callus during sugarcane somatic embryogenesis. PLoS One 10:e0127803

Hsieh CL (2000) Dynamics of DNA methylation pattern. Curr Opin Genet Dev 10:224–228

Huang J, Cardoza YJ, Schmelz EA, Raina R, Engelberth J, Tumlinson JH (2003) Differential volatile emissions and salicylic acid levels from tobacco plants in response to different strains of *Pseudomonas syringae*. Planta 217:767–775

Jacob Y, Martienssen RA (2011) Chromatin reprogramming: gender equality during *Arabidopsis* germline differentiation. Curr Biol 21:R20–R22

Jo L, dos Santos ALW, Bueno CA, Barbosa HR, Floh EIS (2013) Proteomic analysis and polyamines, ethylene and reactive

oxygen species levels of *Araucaria angustifolia* (Brazilian pine) embryogenic cultures with different embryogenic potential. Tree Physiol 34:94–104

Johnston JW, Harding K, Bremner DH, Souch G, Green J, Lynch PT et al (2005) HPLC analysis of plant DNA methylation: a study of critical methodological factors. Plant Physiol Biochem 43:844–853

Karami O, Saidi A (2010) The molecular basis for stress-induced acquisition of somatic embryogenesis. Mol Biol Rep 37:2493–2507

Khan MY, Aliabbas S, Kumar V, Rajkumar S (2009) Recent advances in medicinal plant biotechnology. Indian J Biotechnol 8:9–22

Kitamya E, Suzuki S, Sano T, Nagata N (2000) Isolation of two genes that were induced upon the initiation of somatic embryogenesis on carrot hypocotyls by high concentration of 2,4-D. Plant Cell Rep 19:551–557

Klimaszewska K, Noceda C, Pelletier G, Label P, Rodriguez R, Lelu-Walter M-A (2009) Biological characterization of young and aged embryogenic cultures of *Pinus pinaster* (Ait.). In Vitro Cell Dev Biol-Plant 45:20–33

Klimaszewska K, Overton C, Stewart D, Rutledge RG (2011) Initiation of somatic embryos and regeneration of plants from primordial shoots of 10-year-old somatic white spruce and expression profiles of 11 genes followed during the tissue culture process. Planta 233:635–647

Komatsu S, Nanjo Y, Nishimura M (2013) Proteomic analysis of the flooding tolerance mechanism in mutant soybean. J Proteomics 79:231–250

Křeček P, Skůpa P, Libus J, Naramoto S, Tejos R, Friml J et al (2009) The PIN-FORMED (PIN) protein family of auxin transporters. Genome Biol 10:249

Krogan NT, Long JA (2009) Why so repressed? Turning off transcription during plant growth and development. Curr Opin Plant Biol 12:628–636

Lalli PM, Corilo YE, Fasciotti M, Riccio MF, de Sa GF, Daroda RJ et al (2013) Baseline resolution of isomers by traveling wave ion mobility mass spectrometry: investigating the effects of polarizable drift gases and ionic charge distribution. J Mass Spectrom 48:989–997

Lambé P, Mutambel H, Fouché J-G, Deltour R, Foidart J-M, Gaspar T (1997) DNA methylation as a key process in regulation of organogenic totipotency and plant neoplastic progression? In Vitro Cell Dev Biol-Plant 33:155–162

Latijnhouwers M, Xu XM, Møller SG (2010) *Arabidopsis* stromal 70-kDa heat shock proteins are essential for chloroplast development. Planta 232:567–578

Leljak-Levanic D, Mihaljevic S, Jelaska S (2009) Variations in DNA methylation in *Picea omorika* (Panc) purk. Embryogenic tissue and the ability for embryo maturation. Propag Ornam Plants 9:3–9

LoSchiavo F, Pitto L, Giuliano G, Torti G, Nuti-Ronchi V, Marazziti D et al (1989) DNA methylation of embryogenic carrot cell cultures and its variations as caused by mutation, differentiation, hormones and hypomethylating drugs. Theor Appl Genet 77:325–331

Luge T, Kube M, Freiwald A, Meierhofer D, Seemüller E, Sauer S (2014) Transcriptomics assisted proteomic analysis of *Nicotiana occidentalis* infected by *Candidatus* Phytoplasma mali strain AT. Proteomics 14:1882–1889

Marsoni M, Bracale M, Espen L, Prinsi B, Negri AS, Vannini C (2008) Proteomic analysis of somatic embryogenesis in *Vitis vinifera*. Plant Cell Rep 27:347–356

Miguel C, Marum L (2011) An epigenetic view of plant cells cultured in vitro: somaclonal variation and beyond. J Exp Bot 62:3713–3725

Minocha SC, Minocha R (1995) Role of polyamines in somatic embryogenesis. In: Bajaj YPS (ed) Biotechnology in agriculture and forestry: somatic embryogenesis and synthetic seed 1. Springer, Berlin, pp 53–70

Morano KA, Grant CM, Moye-Rowley WS (2012) The response to heat shock and oxidative stress in *Saccharomyces cerevisiae*. Genetics 190:1157–1195

Msogoya TJ, Grout BW, Roberts A (2011) Reduction in genome size and DNA methylation alters plant and fruit development in tissue culture induced off-type banana (*Musa* spp.). J Anim Plant Sci 3:1450–1456

Noceda C, Salaj T, Pérez M, Viejo M, Cañal MJ, Salaj J et al (2009) DNA demethylation and decrease on free polyamines is associated with the embryogenic capacity of *Pinus nigra* Arn. cell culture. Trees 23:1285–1293

Padmanabhan V, Dias DM, Newton RJ (1997) Expression analysis of a gene family in loblolly pine (*Pinus taeda* L.) induced by water deficit stress. Plant Mol Biol 35:801–807

Pan ZY, Guan R, Zhu SP, Deng XX (2009) Proteomic analysis of somatic embryogenesis in Valencia sweet orange (*Citrus sinensis* Osbeck). Plant Cell Rep 28:281–289

Pan ZY, Zhu SP, Guan R, Deng XX (2010) Identification of 2,4-D-responsive proteins in embryogenic callus of Valencia sweet orange (*Citrus sinensis* Osbeck) following osmotic stress. Plant Cell Tiss Org Cult 103:145–153

Panza V, Lainez V, Maroder H, Prego I, Maldonado S (2002) Storage reserves and cellular water in mature seeds of *Araucaria angustifolia*. Bot J Linn Soc 140:273–281

Poethig RS (1990) Phase change and the regulation of shoot morphogenesis in plants. Science 250:923–930

Rival A, Ilbert P, Labeyrie A, Torres E, Doulbeau S, Personne A et al (2013) Variations in genomic DNA methylation during the long-term in vitro proliferation of oil palm embryogenic suspension cultures. Plant Cell Rep 32:359–368

Rodríguez-López CM, Wetten AC, Wilkinson MJ (2010) Progressive erosion of genetic and epigenetic variation in callus-derived cocoa (*Theobroma cacao*) plants. New Phytol 186:856–868

Rose JKC, Bashir S, Giovannoni JJ, Jahn MM, Saravanan RS (2004) Tackling the plant proteome: practical approaches, hurdles and experimental tools. Plant J 39:715–773

Ruiz-García L, Cervera MT, Martínez-Zapater JM (2005) DNA methylation increases throughout *Arabidopsis* development. Planta 222:301–306

Salmen-Espindola L, Noin M, Corbineau F, Come D (1994) Cellular and metabolic damage induced by desiccation in recalcitrant *Araucaria angustifolia* embryos. Bot J Linn Soc 140:273–281

Sang YL, Xu M, Ma FF, Chen H, Xu XH, Gao XQ et al (2012) Comparative proteomic analysis reveals similar and distinct features of proteins in dry and wet stigmas. Proteomics 12:1983–1998

Santos ALW, Silveira V, Steiner N, Vidor M, Guerra MP (2002) Somatic embryogenesis in Paraná Pine (*Araucaria angustifolia* (Bert.) O. Kuntze). Braz Arch Biol Technol 45:97–106

Santos ALW, Steiner N, Guerra MP, Zoglauer K, Moerschbacher BM (2008) Somatic embryogenesis in *Araucaria angustifolia*. Biol Plant 52:195–199

Santos ALW, Silveira V, Steiner N, Maraschin M, Guerra MP (2010) Biochemical and morphological changes during the growth kinetics of *Araucaria angustifolia* suspension cultures. Braz Arch Biol Technol 53:497–504

Sghaier-Hammami B, Jorrín-Novo JV, Gargouri-Bouzid R, Drira N (2010) Abscisic acid and sucrose increase the protein content in date palm somatic embryos, causing changes in 2-DE profile. Phytochemistry 71:1223–1236

Stasolla C, Yeung EC (2003) Recent advances in conifer somatic embryogenesis: improving somatic embryo quality. Plant Cell Tiss Org Cult 74:15–35

Teyssier C, Maury S, Beaufour M, Grondin C, Delaunay A, Le Metté C et al (2014) In search of markers for somatic embryo maturation in hybrid larch (*Larix* × *eurolepis*): global DNA methylation and proteomic analyses. Physiol Plant 150:271–291

Valledor L, Hasbún R, Meijón M, Rodríguez J, Santamaría E, Viejo M et al (2007) Involvement of DNA methylation in tree development and micropropagation. Plant Cell Tiss Org Cult 91:75–86

Vieira LN, Santa-Catarina C, Fraga HPF, Santos ALW, Steinmacher DA, Schlögl PS et al (2012) Glutathione improves early somatic embryogenesis in *Araucaria angustifolia* (Bert) O. Kuntze by alteration in nitric oxide emission. Plant Sci 195:80–87

Vuorinen T, Nerg AM, Ibrahim MA, Reddy GVP, Holopainen JK (2004) Emission of *Plutella xylostella*-induced compounds from cabbages grown at elevated CO_2 and orientation behavior of the natural enemies. Plant Physiol 135:1984–1992

Washburn MP, Wolters D, Yates JR (2001) Large-scale analysis of the yeast proteome by multidimensional protein identification technology. Nat Biotechnol 19:242–247

Waters ER, Aevermann BD, Sanders-Reed Z (2008) Comparative analysis of the small heat shock proteins in three angiosperm genomes identifies new subfamilies and reveals diverse evolutionary patterns. Cell Stress Chaperones 13:127–142

Weijers D, Sauer M, Meurette O, Friml J, Ljung K, Sandberg G et al (2005) Maintenance of embryonic auxin distribution for apical-basal patterning by PIN-FORMED–dependent auxin transport in *Arabidopsis*. Plant Cell 17:2517–2526

Yasuda H, Nakajima M, Ito T, Ohwada T, Masuda H (2001) Partial characterization of genes whose transcripts accumulate preferentially in cell clusters at the earliest stage of carrot somatic embryogenesis. Plant Mol Biol 45:705–712

Yu Y-Q, Gilar M, Lee PJ, Bouvier ES, Gebler JC (2003) Enzyme-friendly, mass spectrometry-compatible surfactant for in-solution enzymatic digestion of proteins. Anal Chem 75:6023–6028

Zarsky V, Garrido D, Eller N, Tupy J, Vicente O, Schöffl F et al (1995) The expression of a small heat shock gene is activated during induction of tabacco pollen embryogenesis by starvation. Plant Cell Environ 18:139–147

Zhang CX, Li Q, Kong L (2007) Induction, development and maturation of somatic embryos in Bunge's pine (*Pinus bungeana* Zucc. ex Endl.). Plant Cell Tiss Org Cult 91:273–280

Zhang W, Zhou RG, Gao YJ, Zheng SZ, Xu P, Zhang SQ et al (2009) Molecular and genetic evidence for the key role of AtCaM3 in heat-shock signal transduction in *Arabidopsis*. Plant Physiol 149:1773–1784

Zhang C-C, Yuan W-Y, Zhang Q-F (2012) *RPL1*, a gene involved in epigenetic processes regulates phenotypic plasticity in rice. Mol Plant 5:482–493